

## A microfluidic-based neurotoxin concentration gradient for the generation of an *in vitro* model of Parkinson's disease

Azadeh Seidi,<sup>1</sup> Hirokazu Kaji,<sup>2,3</sup> Nasim Annabi,<sup>4</sup> Serge Ostrovidov,<sup>1</sup> Murugan Ramalingam,<sup>1,5</sup> and Ali Khademhosseini<sup>1,2,6,a)</sup>

<sup>1</sup>WPI-Advanced Institute for Materials Research, Tohoku University, Sendai 980-8577, Japan

<sup>2</sup>Department of Medicine, Center for Biomedical Engineering, Brigham and Women's Hospital, Harvard Medical School, Cambridge, Massachusetts 02139, USA and Harvard-MIT Division of Health Sciences and Technology, Massachusetts Institute of Technology, Cambridge, Massachusetts 02139, USA

<sup>3</sup>Department of Bioengineering and Robotics, Graduate School of Engineering, Tohoku University, Sendai 980-8579, Japan

<sup>4</sup>School of Chemical and Biomolecular Engineering, University of Sydney, Sydney, New South Wales 2006, Australia

<sup>5</sup>Faculte de Medecine, National Institute of Health and Medical Research U977, Université de Strasbourg, Strasbourg, Cedex 67085, France

<sup>6</sup>Wyss Institute for Biologically Inspired Engineering, Harvard University, Boston, Massachusetts 02115, USA

(Received 19 January 2011; accepted 30 March 2011; published online 29 June 2011)

In this study, we developed a miniaturized microfluidic-based high-throughput cell toxicity assay to create an *in vitro* model of Parkinson's disease (PD). In particular, we generated concentration gradients of 6-hydroxydopamine (6-OHDA) to trigger a process of neuronal apoptosis in pheochromocytoma PC12 neuronal cell line. PC12 cells were cultured in a microfluidic channel, and a concentration gradient of 6-OHDA was generated in the channel by using a back and forth movement of the fluid flow. Cellular apoptosis was then analyzed along the channel. The results indicate that at low concentrations of 6-OHDA along the gradient (i.e., approximately less than 260  $\mu\text{M}$ ), the neuronal death in the channel was mainly induced by apoptosis, while at higher concentrations, 6-OHDA induced neuronal death mainly through necrosis. Thus, this concentration appears to be useful for creating an *in vitro* model of PD by inducing the highest level of apoptosis in PC12 cells. As microfluidic systems are advantageous in a range of properties such as throughput and lower use of reagents, they may provide a useful approach for generating *in vitro* models of disease for drug discovery applications. © 2011 American Institute of Physics. [doi:10.1063/1.3580756]

### I. INTRODUCTION

Parkinson's disease (PD) is one of the most important neurodegenerative disorders, affecting over 1 million people in the U.S. alone.<sup>1,2</sup> The death of dopaminergic neurons of the substantia nigra (SN) pars compacta,<sup>3</sup> together with accumulation of  $\alpha$ -synuclein inclusions known as Lewy bodies in the SN,<sup>4</sup> constitutes the major neuropathological hallmarks of PD.<sup>5</sup> 6-hydroxydopamine (6-OHDA), a hydroxylated analog of dopamine, is a neurotoxic agent that can be used to selectively damage dopaminergic neurons *in vivo* and *in vitro*, and create animal models of PD.<sup>6</sup> 6-OHDA is uptaken by dopaminergic neurons through the dopamine transporter, and causes oxi-

<sup>a)</sup> Author to whom correspondence should be addressed. Tel.: +1-617-388-9271. FAX: +1-617-768-8477. Electronic mail: alik@rics.bwh.harvard.edu.

ductive damage of mitochondria via free radical-induced lipid peroxidation.<sup>7</sup> The creation of PD animal models using 6-OHDA has led to elucidation of molecular events involved in the progress of PD. The drugs designed so far to treat PD have been relatively effective, especially in the early stages of the disease. However, these drugs do not offer an ultimate cure for the disease and generate side effects such as involuntary movements (called dyskinesia).<sup>8</sup> Therefore, the identification of new drugs with enhanced therapeutic potential is of benefit for the treatment of PD.

High-throughput screening (HTS) assays enable researchers to conduct a large number of tests for screening the efficiency of a drug and its effective concentration to exert the desired effect on the target molecule associated with a particular disease.<sup>9</sup> Cytotoxicity assays employing HTS test the effect of multiple concentrations of a drug usually by means of a multiwell plate cell culture system. However, the use of conventional HTS for cell-based drug screening has certain limitations. For example, high cost of making such assays for the rapid screening of expensive drugs.<sup>10</sup> Therefore, there is a need for new strategies to provide HTS with the minimal experimental variability, and costs.

Microfluidic devices have been extensively used for high-throughput medical assays.<sup>11,12</sup> Generation of drug concentration gradients through microfabrication technology has been used as an advantageous analytical tool for the application of drug screening and cytotoxicity testing.<sup>13–17</sup> This approach provides a miniaturized high-throughput analytical tool that could bypass the problems of using animals for studying the effects of drugs and toxins. It can also minimize the cost, time, sample size requirements, and ethical and legal concerns associated with animal or human use by exposing cells to drug concentrations, which span a few orders of magnitude.<sup>13,18</sup> Chemical concentration gradients can be used to generate a dose-response curve, in a single experiment. For example, Tirella *et al.* developed a microfluidic gradient maker to analyze the dose-dependent effect of bupivacaine and lidocaine anesthetics on C2C12 myoblasts.<sup>13</sup> They designed a microfluidic device with laminar flow within microchannels to create a continuous concentration gradient in the culture chamber. The gradient microfluidic device was found to be a more sensitive method for the detection of cell toxicity compared with conventional multiwell HTS assays as it required a single cell culture exposed to a variety of continued anesthetic gradients. However, the shear stress on cells affected the efficiency of this system. Du *et al.* generated a portable microfluidic device in which the formation of a cardiac toxin, alphacypermethrin, concentration gradient along the microchannel was created initially by a passive-pump-induced forward flow, followed by an evaporation-induced backward flow.<sup>14</sup> Using this technique, a centimeter-long gradient of the toxin was created within 10 min, which was stabilized by stopping the flow. This system was used to test the response of HL-1 cardiac cells to a toxin gradient in the microfluidic device. Although the simplicity and portability of this system were suitable for reliable drug screening applications, this method of gradient generation is not fast enough for minimizing the exposure of cells to drugs such as 6-OHDA.<sup>19</sup>

The aim of this study was to develop a microfluidic-based HTS system to optimize the concentration of 6-OHDA for creation of an *in vitro* model of PD. This system was used to detect and quantify the apoptosis in the pheochromocytoma (adrenal gland tumor) neuronal cell line PC12. Due to the oxidation of 6-OHDA within a short time, in this study, we developed an accelerated method of generating 6-OHDA concentration gradients in a microfluidic device, based on fluid flow movement due to back and forth pumping of fluids inside the channel. The cells were cultured in a microfluidic channel, and a concentration gradient of neurotoxin was generated in the channel using the repeated forward and backward fluid movements. The neuronal cell viability along the channel was observed to vary in a graded way to be lowest at the region with the highest concentration of neurotoxin. The mechanism of cell death was also proved to be dependent on 6-OHDA concentration. The concentration gradient of 6-OHDA used in this study may be useful for determining the optimal toxin concentration required for the neuronal apoptosis to create a PD model in a single experiment with minimized experimental variability. This simple method provides a fast, inexpensive, and efficient platform, as an alternative to animal models, for drug discovery and drug screening.

## II. MATERIALS AND METHODS

### A. Materials

PC12 cells were obtained from RIKEN Bioresource Center Cell Bank, Japan. 6-OHDA (MW: 205.6), poly-L-lysine (PLL) hydrobromide, and penicillin/streptomycin were purchased from Sigma, USA. Fluorescein isothiocyanate-Dextran (FITC-Dextran, MW: 10 kD) and sodium metabisulfite were purchased from Sigma-Aldrich. Fetal bovine serum (FBS) was purchased from Japan Bioserum. Phosphate buffered saline (PBS), Dulbecco's Modified Eagle medium (DMEM) and horse serum were purchased from Gibco, NZ. Live/dead assay kit was purchased from Invitrogen, USA. Annexin V-FITC apoptosis kit was purchased from Abcam, Japan. Polydimethylsiloxane (PDMS) prepolymer and the curing agent (Silpot 184 kit) were purchased from Dow Corning Toray, Japan.

### B. Determination of 6-OHDA oxidation

The oxidation of 6-OHDA at various concentrations in an oxygen-containing medium (i.e., PBS) was determined by using spectrophotometric analysis. The stock solution of 6-OHDA (10 mM) was prepared in nitrogen-bubbled MilliQ, containing 0.1% sodium metabisulfite as an antioxidant. The experiment was initiated by the addition of 6-OHDA at the final concentrations of 0, 100, 200, 300, 400, 500, 800, and 1000  $\mu\text{M}$  to 96-well plate containing PBS (total volume: 200  $\mu\text{L}$ ). The temperature of the plate reader (BioTek Synergy HT) was set at 37 °C to correspond to cellular 6-OHDA treatment. Maximum absorption of p-quinone (490 nm) was monitored every min for 1 h using the plate reader.

### C. Fabrication of the microfluidic device

The microfluidic device was fabricated by using a standard soft lithographic method described previously.<sup>20</sup> Briefly, PDMS molds were fabricated by curing prepolymer of silicone elastomer and curing agent (10:1 ratio). The PDMS prepolymer was poured on a silicon master that was patterned with photoresist, and cured at 70 °C for 1.5 h. PDMS mold was then peeled off from the silicon wafer. For medium perfusion and cell seeding, the inlet and outlet of the microchannel were punctured by sharp punches, with hole diameters of 3 and 5 mm, respectively. The dimension of top fluidic channel was 100  $\mu\text{m}$ (height)  $\times$  30 mm(length)  $\times$  2 mm(width). To generate the channels, the PDMS mold was irreversibly bonded to a glass slide, after plasma treatment (Harrick Scientific, PDC-001).

### D. Generation of concentration gradients in the microfluidic device

The schematic representation of the method to generate a concentration gradient of molecules in a straight microfluidic channel is illustrated in Fig. 1. The gradient was generated due to the fluid flow movements during the back and forth pumping of fluids inside the channel using a pipette. The channel was initially filled with solution 1 (e.g., de-ionized water). A 200  $\mu\text{L}$  drop of water was pipetted onto the outlet port and a 20  $\mu\text{L}$  drop of another solution (i.e., solution 2) with a high concentration of the chemical of interest (e.g., a model fluorescent-labeled molecule such as FITC-Dextran) was pipetted into the empty inlet port. The outlet port (diameter: 5 mm) was emptied by taking the excess water with a pipette, without exerting any suction of liquid from the channel by the pipette. This accelerated the fluid flow from the inlet port to the outlet port. When the tip of the forward flow reached near the outlet port, as visualized by tracking FITC-Dextran, it was stopped by returning the 200  $\mu\text{L}$  water drop to the outlet port. A fast backward flow was initiated by reducing the volume of the droplet at the inlet port by taking 10  $\mu\text{L}$  of the liquid with a pipette, which reversed the direction of fluid flow in the channel, and moved the gradient to the inlet side of the channel. The gradient was then stabilized by sealing the inlet and outlet ports with thin slices of cured PDMS.

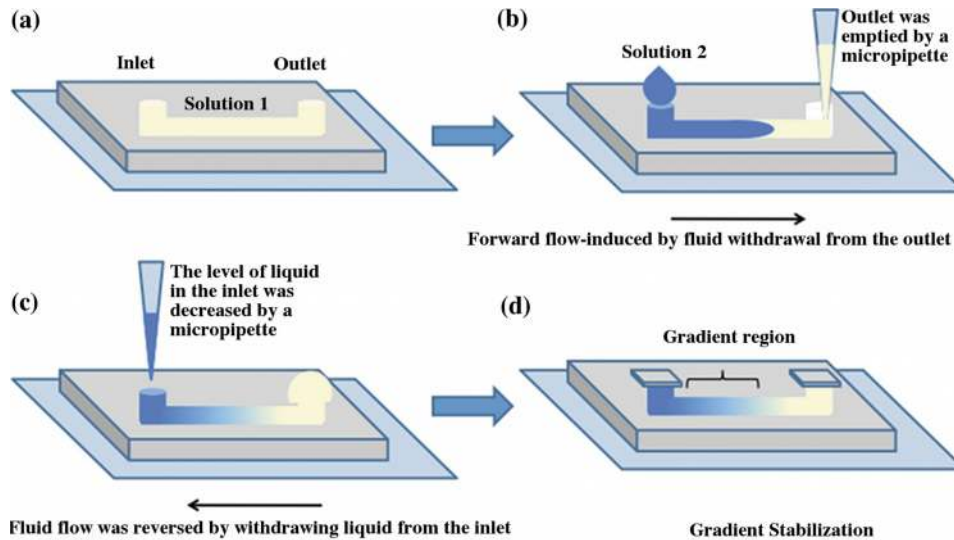


FIG. 1. Schematic of the technique for generation of concentration gradients in a microfluidic channel. (a) Microfluidic channel was first filled with solution 1 (i.e., water or culture medium). (b) Solution 2 (i.e., a fluorescent-labeled molecule or 6-OHDA) was introduced from the inlet, while the removal of the liquid from the outlet caused a rapid forward flow of solution 2 inside the channel. (c) The forward flow was reversed into a backward flow from the inlet by placing a drop of solution 1 on the outlet port and withdrawing  $\sim 10 \mu\text{L}$  of liquid from the inlet, which generated a concentration gradient of solution 2 in the channel. (d) The gradient was stabilized by sealing the inlet and outlet ports by two pieces of cured PDMS.

### E. 6-OHDA treatment of cells inside microfluidic channels

PC12 cells were maintained in a culture medium containing 5% FBS, 10% horse serum, 100 U/mL penicillin, and 100  $\mu\text{g}/\text{mL}$  streptomycin at 37 °C in a humidified incubator with 5%  $\text{CO}_2$  and were passaged twice per week. Prior to seeding the cells into the microchannel, the bottom glass slide was coated with PLL (0.1 mg/mL in sterilized de-ionized water) to enhance cell adhesion in the microfluidic channel. Initially, the top channel was irreversibly bonded to the bottom glass slide, and then 0.1 mg/mL solution of PLL was injected into a channel from the outlet and incubated for a minimum of 3 h. The channel was subsequently rinsed and incubated with sterilized de-ionized water for a minimum of 3 h. Then the de-ionized water was removed from the channel by placing droplets of fresh culture medium on the outlet, which pushed the water to the inlet. The water accumulated in the inlet was taken with a pipette; this process was repeated several times to ensure complete replacement of water with culture medium. To seed the cells into the microfluidic device, the cells were trypsinized and seeded through the outlet at the cell density of  $4 \times 10^6$  cells/mL. The cell seeded device was kept in a  $\text{CO}_2$  incubator overnight to ensure cellular attachment in the microchannel. The medium was then changed and a gradient of 6-OHDA was generated in the channel using a neurotoxin solution with a concentration of 1000  $\mu\text{M}$ . The stock solutions of 6-OHDA were freshly prepared for every experiment by dissolving the 6-OHDA powder in a nitrogen-bubbled MilliQ, containing 0.1% sodium metabisulfite as antioxidant, at the final concentration of 10 mM 6-OHDA. To visualize the gradient formation, trypan blue (MW: 960.82), which has a comparable molecular weight (thus, diffusion coefficient) to that of 6-OHDA, was added to 6-OHDA solution at the final concentration of 0.025 wt %. A control gradient of trypan blue was generated to rule out the possibility of cytotoxicity from this dye. After gradient formation and stabilization by sealing the inlet and outlet ports with PDMS pieces, the microfluidic device was transferred to the cell culture incubator. The cellular assessments were performed after 24 h incubation. In order to eliminate the possibility of cellular apoptosis as a result of nutrient deprivation, the culture media in the channel were changed at the end of 6-OHDA active life time.

## F. 6-OHDA treatment of cells in multiwells

A conventional cytotoxicity assay in a multiwell system was performed in order to determine the dose-dependent effect of 6-OHDA on PC12 cell viability, and to compare the cytotoxicity of 6-OHDA in two systems (i.e., gradient system and multiwell system). PC12 cells were cultured in PLL-coated 8-well Laboratory Tek chamber slides for 24 h at the density of  $1 \times 10^5$  cells/cm<sup>2</sup>. The media were then changed, and 6-OHDA was added to cells at the final concentrations ranging from 0 to 1000  $\mu$ M from the freshly prepared 10 mM stock solution in cell culture media. The chamber slides were then incubated at 37 °C for 24 h to treat the cells with 6-OHDA.

## G. Viability assay

The cytotoxicity of 6-OHDA on PC12 cells was determined using a live/dead kit consisting of calcein AM and ethidium homodimer-1 (EthD-1), which can be used to distinguish live cells from dead cells. Calcein AM is nonfluorescent cell-permeable molecule, which is converted into highly fluorescent calcein (ex/em  $\sim$ 495 nm/ $\sim$ 515 nm) through ubiquitous intracellular esterase activity in live cells. EthD-1 can only be uptaken by dead cells with damaged plasma membranes, and binds the nucleic acids. This phenomenon causes a 40-fold enhancement of fluorescence (ex/em  $\sim$ 495 nm/ $\sim$ 635 nm). Using a fluorescence microscope (Carl Zeiss, Observer Z1), live cells stained with calcein were visualized by an intense green color, while dead cells stained with EthD-1 were visualized by a bright red color.

## H. Assessment of apoptosis and necrosis

The extent of apoptosis and necrosis was assessed by staining annexin V-FITC and propidium iodide (PI) staining. In the early stages of apoptosis, phosphatidyl-serine (PS) translocates from the inner face of the plasma membrane to the outer leaflet. Annexin V binds to PS, and can be used to detect cells at the early stages of apoptosis.<sup>21</sup> The combination of annexin V-FITC and PI staining can identify the late stages of apoptosis, due to the loss of membrane integrity at this stage, while necrotic cells can be detected by staining with PI alone. PC12 cells treated with 6-OHDA were stained with annexin V-FITC/PI for 5 min, followed by fixation in 2% paraformaldehyde (30 min, room temperature) and staining with 4',6-diamidino-2-phenylindole (DAPI) (1.5  $\mu$ g/ml, 10 min, and 37 °C). Fluorescent images were used to quantify the rate of apoptotic and necrotic cells in total cell populations.

## III. RESULTS AND DISCUSSION

### A. Evaluation of dose-dependent effect of 6-OHDA on H<sub>2</sub>O<sub>2</sub> production and cell viability

6-OHDA rapidly oxidizes in the presence of oxygen and yields H<sub>2</sub>O<sub>2</sub> and p-quinone, which induces apoptosis upon being uptaken by cells.<sup>19</sup> The inactivation of toxin can be characterized by the color change of 6-OHDA solution into pink, caused by generation of p-quinone.<sup>22</sup> In this study, the formation of p-quinone was quantified in a cell-free system by measuring the solution absorbance at 490 nm over time in order to determine the degradation time of 6-OHDA in an oxygen-containing solution, such as PBS. As indicated in Fig. 2(a), the stock solution of 6-OHDA was stable during the measurement time, while the oxidation reaction in PBS containing wells was completed within 5–40 min for various concentrations of 6-OHDA. The profile of p-quinone production at low concentrations of 6-OHDA (i.e., 100–400  $\mu$ M) exhibited an immediate increase in the level of p-quinone upon addition of toxin to PBS, which continued up to 3 min and then reached a plateau. This confirmed the complete oxidization of 6-OHDA within 2–3 min at low concentrations. However, at high concentrations of 6-OHDA (i.e., 500–1000  $\mu$ M), the oxidation reaction started 5 min after the addition of toxin to PBS. At this point, the oxidation reaction accelerated sharply as evidenced by the increase in absorption at 490 nm. This trend continued for  $\sim$ 20–40 min, depending on the toxin concentration, after which the absorption level remained constant. This lag time ( $\sim$ 5 min) at highly concentrated samples may be attributed

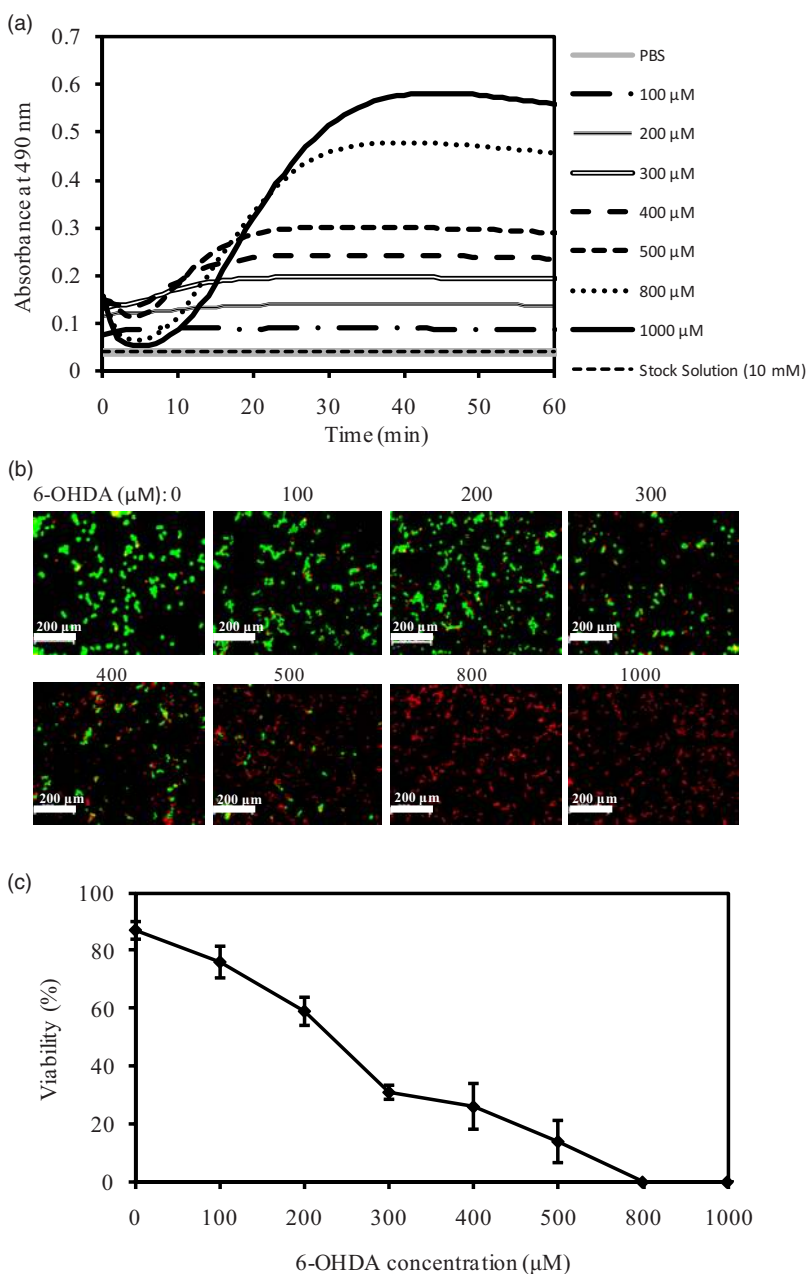


FIG. 2. The effect of 6-OHDA on  $\text{H}_2\text{O}_2$  generation and PC12 cell viability. (a) The oxidation of 6-OHDA at various concentrations was measured spectrophotometrically at 37  $^\circ\text{C}$  every minute for 1 h. The formation of p-quinone was monitored at 490 nm in the PBS. (b) Live/dead staining of PC12 cells cultured in Lab-Tek 8-well chamber slides at the density of  $10^5$  cell/ $\text{cm}^2$  and treated for 24 h with 0, 100, 200, 300, 400, 500, 800, and 1000  $\mu\text{M}$  6-OHDA (scale: 200  $\mu\text{m}$ ). (c) The quantification of cell viability by counting the live and dead cells using IMAGEJ. Each value is the average cell viability  $\pm$  SD from three images taken from the cells in each well.

to higher fraction of 6-OHDA stock solution, containing antioxidant, in the corresponding wells, which resulted in a temporary protection of 6-OHDA molecules against oxidation. This result indicated that the addition of 6-OHDA to an oxygen-containing medium initiated the production of harmful reaction species, which can cause cellular apoptosis, until the complete degradation of neurotoxin. Consequently, control over the exposure time of 6-OHDA to oxygen is a crucial factor in order to optimize toxin treatment condition.

The  $\text{H}_2\text{O}_2$ , produced through oxidation of 6-OHDA, generates hydroxyl radicals by reacting with transition metals such as iron in cells. Hydroxyl radicals immediately react with lipids, DNA, and amino acids in proteins to damage cells.<sup>23</sup> Oxidative production of  $\text{H}_2\text{O}_2$  and quinone has also been shown to inhibit active mitochondrial respiration and to increase mitochondrial swelling and inner membrane permeability.<sup>7</sup> These molecular events contribute to 6-OHDA-induced toxicity, mimicking the neurodegenerative process in PD. To determine the cytotoxic effect of 6-OHDA on PC12 cells, the cells were cultured in an 8-well Lab-Tek chamber slide for 24 h to ensure attachment before treatment with 6-OHDA. Cell viability was assessed by the addition of calcein AM and EthD-1 to the chamber slides. PC12 cells treated with various amounts of 6-OHDA for 24 h exhibited a decrease in viability in a dose-dependent manner [Figs. 2(b) and 2(c)]. The images of cells stained with calcein AM and EthD-1, together with quantified viability values, indicated that the median lethal dose ( $\text{LD}_{50}$  value) of 6-OHDA is around  $230 \mu\text{M}$ , while 6-OHDA concentrations higher than  $800 \mu\text{L}$  resulted in a complete cell death [Fig. 2(b)]. Saito *et al.* studied the dose-dependent effect of 6-OHDA on PC12 cell viability.<sup>24</sup> In this study, complete cell death was observed when the cells were treated with  $100 \mu\text{M}$  concentration of 6-OHDA for 24 h.<sup>24</sup> However, Jin *et al.* reported only  $\sim 20\%$  decrease in PC12 cell viability under the same condition.<sup>25</sup> The difference in the efficiency of the toxin in these studies can be attributed to the oxidation of 6-OHDA, which may result in its deactivation in the medium. Due to the observation of complete cell death at toxin concentration of  $1000 \mu\text{M}$ , this concentration was used to generate toxin concentration gradients in microfluidic devices.

## B. Generation of the concentration gradient of FITC-Dextran in the microfluidic channel

The system illustrated in Fig. 1 was used to generate a concentration gradient, which was stable during the oxidation time of 6-OHDA. The efficiency of the system was evaluated by using FITC-Dextran. The microfluidic channel was initially filled with de-ionized water after which a  $200 \mu\text{L}$  drop of de-ionized water was pipetted onto the outlet. A  $20 \mu\text{L}$  drop of FITC-Dextran ( $1.5 \times 10^{-4} \text{ M}$ ) was then pipetted onto the emptied inlet. A passive-pump-induced forward flow was used to direct FITC-Dextran into the channel,<sup>26</sup> and the flow was accelerated by taking the excess liquid from the outlet port. The use of accelerated pumping of liquids through the microfluidic channel in this study decreased the duration of forward flow from 3 min (achieved based on passive pumping alone) to 3–5 s. This time was long enough for the FITC-Dextran droplet to reach near the end of the channel. At this point, the liquid was pipetted back onto the outlet to guide the fluid flow to the opposite direction. The speed of the backward flow was also increased by taking the excess liquid from the inlet, which decreased the time required for the backward flow to generate a concentration gradient from 10 min to 10–15 s. The total time required for gradient generation and stabilization was less than 30 s; this can be advantageous for generation of a concentration gradient of unstable chemicals such as 6-OHDA that undergo structural changes upon being exposed to oxygen-containing environments. The profile of the centimeter-long concentration gradient of FITC-Dextran was quantified by measuring the fluorescent intensity along the channel for 1 h at various time points after the generation of the gradient [Figs. 3(a) and 3(b)]. The results indicated that the gradient profile had an acceptable stability during the oxidation time of 6-OHDA (i.e.,  $\sim 40$  min).

It is crucial to estimate the 6-OHDA distribution along the channel and to correlate the cellular response to the toxin concentration in order to use the gradient channel for testing a range of 6-OHDA concentrations. In this study, a standard curve was plotted to convert fluorescence intensity values to FITC-Dextran concentrations (data not shown). The length of the channel was divided into six regions, each with a 0.5 cm length, and the fluorescence intensity values were used to estimate the mean concentration of FITC-Dextran in each region [Fig. 3(c)]. The mean concentration of FITC-Dextran at various regions within the channel was estimated by calculating the mean fluorescence intensity along each region during the first 40 min after the generation of gradient. The mean concentration values in Fig. 3(b) represented the graded increase in the entire channel. According to the fluorescence intensity profiles, the highest fluorescence intensity in the

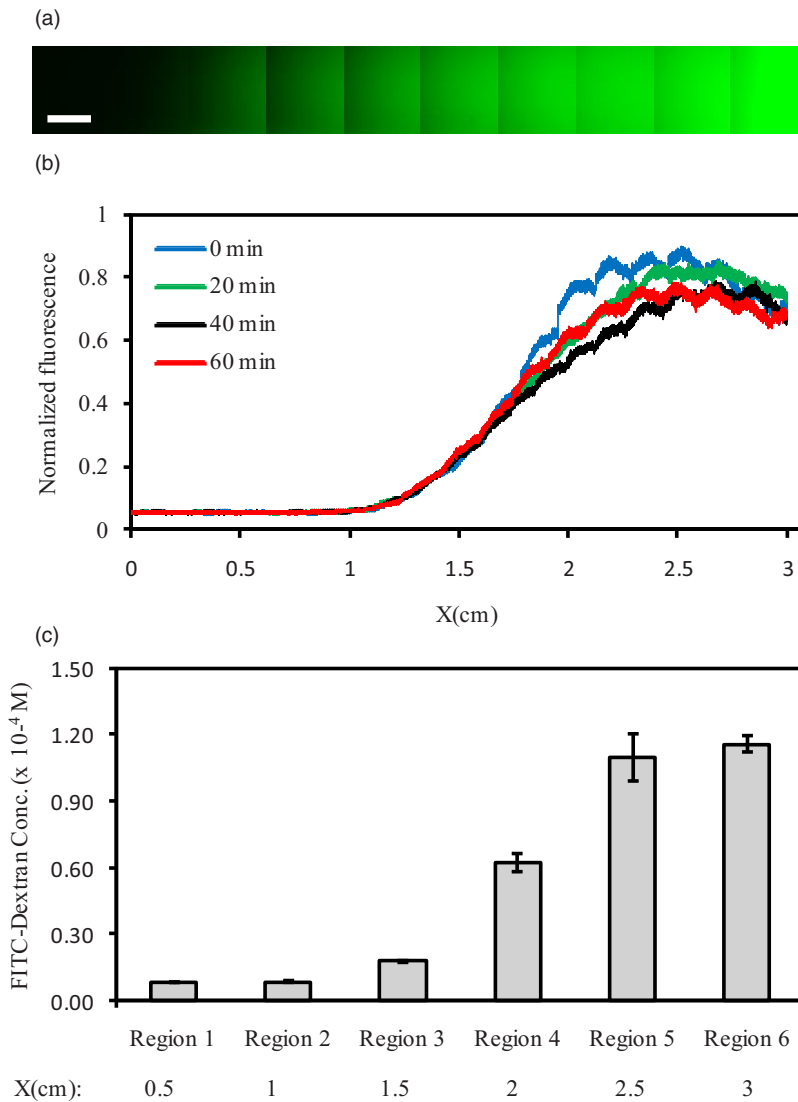


FIG. 3. Characterization of the concentration gradient inside the channel with FITC-Dextran as a model molecule. (a) Fluorescence image of FITC-Dextran (MW: 10 kD) gradient region along the microfluidic channel (scale: 1 mm). (b) Fluorescence intensity profiles were taken along the channel at various time points after the formation of the gradient. The fluorescent intensity values have been normalized to the highest value, which was obtained from the FITC-Dextran solution used as the pumping droplet (concentration:  $1.5 \times 10^{-4}$  M). (c) Concentration gradient of FITC-Dextran distributed along the channel, estimated from fluorescence intensity profiles during the first 40 min after the generation and stabilization of the gradient. Each value was obtained by converting the mean  $\pm$  SD normalized fluorescence intensity along individual regions to FITC-Dextran concentrations. The conversion was performed based on a linear correlation between fluorescence intensity profiles of FITC-Dextran standard solutions in the same channel.

channel, which was normalized to the fluorescence intensity obtained from FITC-Dextran solution used to make gradient, is 0.76. This suggests that FITC-Dextran droplet was diluted due to the mixing with water after entering the channel, and created a concentration gradient, ranging from  $\sim 0\%$  to  $76\%$  of its concentration in the pumping droplet. As shown in Fig. 3(c), FITC-Dextran concentration was increased from  $0.08 \times 10^{-4}$  M in region 1 to  $1.14 \times 10^{-4}$  M in region 6.

### C. Cell viability in microfluidic channels containing 6-OHDA concentration gradients

PC12 cells were cultured in linear microchannels, and a concentration gradient of 6-OHDA was subsequently generated in each channel to demonstrate the efficiency of the system for

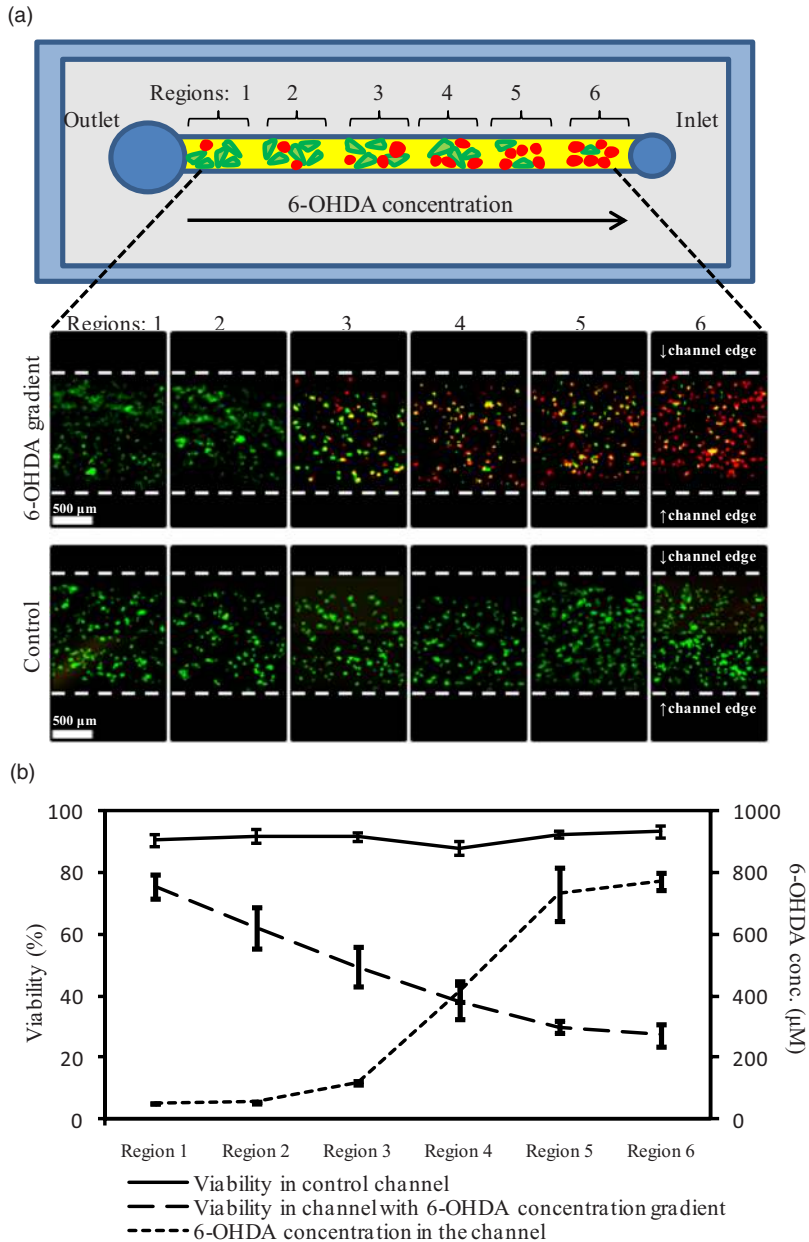


FIG. 4. Graded cell death in the channel with a concentration gradient of 6-OHDA. (a) Representative images of live/dead staining of PC12 cells cultured in microfluidic channel 24 h after exposure to 6-OHDA gradients in the channel with 1000  $\mu\text{M}$  toxin in the pumping droplet (upper panel) or with no added toxin (lower panel) (scale: 500  $\mu\text{m}$ ). (b) Quantification of PC12 viability along the channel with a concentration gradient of 6-OHDA, generated using a toxin solution with 1000  $\mu\text{M}$  concentration. Quantification was performed using IMAGEJ software; each value is the average cell viability  $\pm$  SD in the three consecutive microscope fields of each region (the length of field: 1.7 mm).

generating a graded cell viability along the microfluidic device. The viability of cells along the channels was determined using a live/dead assay. As shown in Fig. 4(a), a gradient in cell viability was obtained along the channels upon exposure to a concentration gradient of 6-OHDA, which ranged between 75% and 27% [Fig. 4(b)]. Based on the distribution profile of FITC-Dextran in the channel [Fig. 3(b)], the concentration of 6-OHDA in the channel was in the range of  $\sim 0$  to 760  $\mu\text{M}$ . As shown in Fig. 4(b), cell viability along the channel was decreased by increasing the mean 6-OHDA concentration in each region; for example, the viability decreased from 75.3% to

27.3% when the mean concentration of 6-OHDA increased from around 0 to 760  $\mu\text{M}$ . In contrast, the average cell viability in the control channel, without toxin treatment, remained unchanged along the channel. The difference in the lowest cell viabilities from the multiwell in Fig. 2(c) and gradient systems can be attributed to the dilution of the 6-OHDA solution upon mixing with the medium in the channel. Another reason can be the difference in the molecular weights of FITC-Dextran (MW: 10 000) and 6-OHDA (MW: 205.6), which caused different values of molecular diffusivity in the channel. Molecular diffusivities of FITC-Dextran and 6-OHDA have been estimated to be  $1.7 \times 10^{-6}$  and  $0.6 \times 10^{-5}$   $\text{cm}^2/\text{s}$ , respectively.<sup>14,27</sup> Although sealing the inlet and outlet ports of the channel stopped the flow, spreading of molecules continued in the channel due to molecular diffusion. Simulation studies in microfluidic gradient generators have previously shown that for large molecules with small diffusion coefficient, the effect of molecular diffusion on the concentration profile is not significant and the concentration profile is fairly stable; while for small molecules with large diffusion coefficient, molecular diffusion has a significant role in mixing of fluid and flattening of the concentration profile in the channel.<sup>13,14,28</sup> It is therefore expected that due to small molecular weight of 6-OHDA, and consequently its high diffusive mixing in the channel, the effective concentration range of the molecule in the channel is lower than FITC-Dextran. The moving length of a gradient in a channel, due to molecular diffusion, can be scaled as  $(\pi t D)^{1/2}$ , where  $D$  is the molecular diffusivity of the molecule, and  $t$  is time.<sup>14</sup> The moving lengths of 6-OHDA and FITC-Dextran gradients during the complete oxidation time of 6-OHDA at 800  $\mu\text{M}$  concentration [i.e., 30 min; Fig. 2(a)] were therefore 2.25 and 1.2 mm, respectively. However, as oxidation of 6-OHDA proceeds, the amount of active toxin may decrease in all regions of the channel with both high and low 6-OHDA concentrations. Therefore, it was assumed that the effect of gradient movement along the channel was negligible. This assumption is favored by the consistency of PC12 viability after 6-OHDA treatment in the multiwell, and gradient system in which the concentration of 6-OHDA in the channel was estimated by using the concentration profile of FITC-Dextran. For example, as shown in Fig. 4(b), region 3 of the channel with the average toxin concentration of  $\sim 118$   $\mu\text{M}$  6-OHDA contained 50% viable cells. While the average toxin concentration values plotted in Fig. 4(b) were helpful to approximately compare the toxin concentration in each region, it should be noted that due to the existence of a toxin concentration gradient in the channel, the actual concentration of 6-OHDA changed in a graded way along each region. According to the FITC-Dextran intensity profiles in the channel [Fig. 3(b)], the concentration of 6-OHDA in region 3 was estimated to vary from 6.5% (at  $X=1$  cm) to 26.2% (at  $X=1.5$  cm) of the concentration in the pumping droplet. Therefore, the concentration of 6-OHDA in this region varies from  $\sim 65$  to  $\sim 260$   $\mu\text{M}$ . The  $\text{LD}_{50}$  value in the multiwell system [Fig. 2(c)] was obtained at  $\sim 230$   $\mu\text{M}$  concentration of 6-OHDA, which is consistent with cell viability in microfluidic-based gradient system. No major cell loss was observed inside the channel due to the detachment of dead cells. In an example of toxicity testing using a microfluidic gradient maker with a continuous flow of medium and toxin, Tirella *et al.* reported a major cell loss as the result of detachment of dead cells due to the presence of shear force exerted by the continuous flow in the system.<sup>13</sup> The static system of cell treatment with a gradient of 6-OHDA in this study could minimize the errors in cell viability values, obtained when using systems with continuous flows.

#### D. Mechanism of cell death in response to the 6-OHDA gradients

The death of dopaminergic neurons in PD occurs by apoptosis.<sup>29</sup> While 6-OHDA has been used to induce apoptosis *in vitro* and *in vivo*, it has been shown to cause neuronal death through two distinct mechanisms: apoptosis and necrosis.<sup>30</sup> Ochu *et al.* studied the survival rate of PC12 cells treated with various amounts of 6-OHDA in conjunction with an apoptosis inhibitor called zVAD-fmk. This study demonstrated that at lower concentrations of 6-OHDA, zVAD-fmk could prevent apoptotic morphology, while at higher concentrations of 6-OHDA, it did not exert such an effect. This means that the mechanism of 6-OHDA-induced neuronal death is highly dependent on its concentration. Therefore, it is crucial to optimize the treatment of PC12 cells with 6-OHDA in

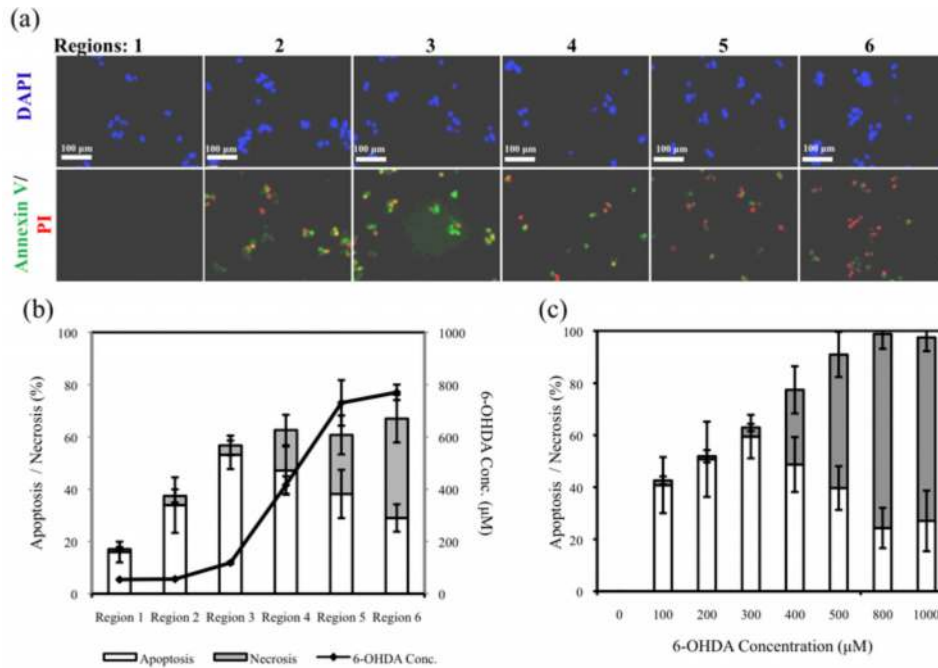


FIG. 5. Assessment of 6-OHDA-induced apoptotic and necrotic PC12 cell death. (a) PC12 cells were cultured in the channel and treated with a concentration gradient of 6-OHDA, with 1000  $\mu\text{M}$  toxin in the pumping droplet, and cultured for 24 h before being costained with annexin V-FITC/PI/DAPI to detect the apoptotic and necrotic cells (scale: 100  $\mu\text{m}$ ). (b) Quantification of 6-OHDA-induced apoptosis and necrosis along a channel with a concentration gradient of 6-OHDA. Data shown are representative of mean value  $\pm$  SD of six images taken from the cells in each region. (c) Comparative study of 6-OHDA-induced PC12 apoptosis and necrosis obtained by a Lab-Tek 8-well chamber slide. Cells were treated with various concentrations of 6-OHDA for 24 h and costained with annexin V-FITC/PI/DAPI to assess the apoptosis and necrosis. Results are represented as mean  $\pm$  SD of at least three images taken from each well.

order to generate the *in vitro* model of this disease, so that the highest rate of apoptosis and the minimum rate of necrosis are achieved.

To optimize the 6-OHDA concentration for generating an *in vitro* model of PD, PC12 cells were cultured in a PLL-coated channel at the density of  $4 \times 10^6$  cells/ml. The culture medium was then changed and a concentration gradient of 6-OHDA was generated in the channel using a freshly prepared 6-OHDA stock solution. The concentration of 6-OHDA in the pumping droplet was 1000  $\mu\text{M}$ , and the gradient generation was visualized by trypan blue (final concentration: 0.025% wt%). After 9 h of treatment with the toxin gradient, the medium was changed and the culture was continued for 24 h. The cells were stained by annexin V-FITC, PI, and DAPI, and subsequently analyzed using a fluorescence microscope [Fig. 5(a)]. The nuclei of cells were stained with DAPI (upper panel, blue stains). Cells undergoing apoptosis were stained with annexin V-FITC (lower panel, green stains), and cells that had lost membrane integrity were stained with PI (lower panel, red stains). As shown in Fig. 5(a), the cells in the early stages of apoptosis exposed PS to the outer leaflet, while maintaining membrane integrity [annexin V-FITC(+)/PI(-)]. In the late stages of apoptosis, the cellular membrane integrity was lost [annexin V-FITC(+)/PI(+)]. In the case of necrosis, ultimate breakdown of the membrane was observed [annexin V-FITC(-)/PI(+)]. We analyzed the percentage of apoptotic and necrotic cells at different stages along the channel [Fig. 5(b)]. As indicated in Fig. 5(b), the percentage of apoptotic cells increased from 15.8% at region 1 of the channel to 53.2% at region 3. However, the percentage of necrotic cells increased only from 1.1% at region 1 to 3.5% at region 3. This means that apoptosis was the major cause of cell death up to region 3 in the channel. This trend changed at the regions which were closer to the inlet port (i.e., regions 4–6) with higher concentrations of 6-OHDA. At these regions, necrosis had a major role in cell death. According to the FITC-Dextran

intensity profiles in the channel [Fig. 3(b)], the value of toxin concentration in the region 3 of the channel was between  $\sim 65$  and  $\sim 260 \mu\text{M}$ . Consequently, at toxin concentrations higher than  $260 \mu\text{M}$ , necrosis started to take the major role in neuronal death. This study clearly demonstrated a distinction between the cellular process of apoptosis and necrosis during PC12 cell death with respect to neurotoxin gradient. These results were consistent with previous studies on the effect of high concentrations of neurotoxins on neuronal cell viability.<sup>31–33</sup> In these studies, it was reported that neurons exposed to low concentrations of the neurotoxin 1-methyl-4-phenylpyridinium (MPP(+)) went through apoptosis, which was rescued by caspase inhibitors. However, at high concentrations of this drug, neuronal cell death could not be rescued by caspase inhibitors, suggesting that at those concentrations, the neuronal death did not occur due to apoptosis.

The results of a parallel experiment in an 8-well Lab-Tek chamber slide, with various amounts of 6-OHDA, indicated that the maximum percentage of apoptotic cells was achieved at toxin concentrations less than  $300 \mu\text{M}$  [Fig. 5(c)]. The percentage of apoptotic cells was approximately 59%, as compared to 1% in the control well without toxin treatment. At toxin concentrations above  $300 \mu\text{M}$ , necrotic events became more significant and the percentage of apoptotic cells declined [Fig. 5(c)]. The percentage of necrotic cells increased to 70% at  $1000 \mu\text{M}$  of 6-OHDA. These results suggest that apoptosis is induced at lower concentrations of 6-OHDA ( $\leq 300 \mu\text{M}$ ) and necrosis is elevated at higher concentrations of 6-OHDA. This was consistent with the data obtained in the microfluidic channel with a concentration gradient of 6-OHDA.

The maximum percentage of apoptosis in both gradient and multiwell systems (i.e., 53.2% and 59%, respectively) showed an acceptable level of consistency. The rate of neuronal necrosis at high toxin concentrations was more significant in the multiwell system compared to microfluidic device. This can be attributed to the dilution of 6-OHDA upon entering the microfluidic channel due to the mixing with the pre-existing medium or the difference between the molecular weight of 6-OHDA and FITC-Dextran.

PD has been reported to be caused by the progressive death of dopaminergic neurons through apoptosis.<sup>29</sup> Therefore, finding the 6-OHDA concentration that mimics the apoptotic cell death as occurring in PD in an *in vitro* model can be particularly important if the therapeutic potential of an antiapoptotic drug such as a caspase inhibitor is to be investigated for the treatment of PD. Such drugs can rescue the healthy cells from apoptosis, thus keeping the disease from progressing. In this case, the *in vitro* model of the disease can be helpful in judging the effectiveness of the antiapoptotic drug only if it has been carefully designed in terms of the 6-OHDA concentration used to induce cellular apoptosis.

In this study, we introduced a miniaturized system comprised of a microfluidic channel with a concentration gradient of a neurotoxin to analyze the effect of neurotoxin concentration on apoptosis and necrosis rates of neuronal cells. Although the gradient system showed sensitivity and specificity similar to those found in a multiwell system, it had several advantages compared to conventional multiwell system and previously developed microfluidic-based gradient generators,<sup>34–36</sup> including the short time required for gradient generation, low cost, high-throughput bioanalytical assays, and small amount of biological target and drug candidates. The system also offered features such as simplicity of design, portability, and fast operation. This microfluidic platform was used to study the performance of various cytotoxic examinations such as cell viability, cell death, and apoptosis analysis, with potential for real time imaging due to the transparency of the device. Although we reported apoptosis assessment, only by plasma membrane phosphatidylserine externalization, other apoptotic events are feasible to monitor such as morphological alterations and nuclei collapse. This microfluidic device integrates the cell culture, drug treatment, staining, and washing steps into a single device to generate a number of experimental conditions simultaneously and has the potential to investigate multiple parameters to relate drug exposure to apoptosis. It offers a unique platform to characterize various cellular responses in a high-throughput fashion, which is otherwise impossible with conventional methods. The developed system in this study offers promising potentials for future uses in the discovery and HTS of drugs to treat PD. It can also be used to pretreat neuronal cells such as PC12, with a gradient concentration of a candidate drug (e.g., an antiapoptotic drug), before exposing the cells to

6-OHDA with the optimized concentration. Investigating cellular responses to the concentration gradient of the candidate drug can provide useful information on the potential therapeutic effects of the drug prior to clinical experiments.

#### IV. CONCLUSIONS

Microfluidic technology has become an attractive tool in biological research and promises to integrate and miniaturize many bioanalytical processes. This provides an alternative platform for the analysis of biological phenomena such as apoptosis and necrosis. In this study, we examined the concentration-dependent cytotoxic effect of 6-OHDA on PC12 cell viability. The results indicated that cells cultured in the microfluidic channel responded to the 6-OHDA concentration gradient by showing a graded viability along the channel. The cellular response was correlated with the toxin concentration by generating a concentration gradient of FITC-Dextran as a model molecule in the channel. The 6-OHDA concentration-dependent cell viability in the gradient system was consistent with the results obtained from a conventional multiwell system. Both systems suggested an LD<sub>50</sub> value of  $\sim 230 \mu\text{M}$  and exhibited a linear decrease in cell viability with an increase in toxin concentration. Furthermore, the effect of 6-OHDA concentration on the mechanism of neuronal death was investigated using the gradient system. The results indicated that at low concentrations of 6-OHDA, the basic mode of cell death behind 6-OHDA-induced cytotoxicity was apoptosis. However, a high concentration of 6-OHDA resulted in a mixture of apoptosis and necrosis. The accuracy of the gradient screening system was examined by performing a parallel experiment in a multiwell system. Using both systems, the highest rate of cellular apoptosis was achieved when the 6-OHDA concentration was  $\sim 260 \mu\text{M}$ , which fulfills the determining criterion for creation of an *in vitro* model of PD.

Given its low use of reagents and ability to generate gradients of rapidly degrading chemicals, this system is potentially useful in the design of cytotoxicity experiments for a range of drug screening applications.

#### ACKNOWLEDGMENTS

This work was financially supported by the World Premier International Research Center-Advanced Institute for Materials Research (WPI-AIMR). H.K. acknowledges the support from JSPS Fellowship for Research Abroad.

A.S., M.R., and A.K. designed the research; A.S. performed the research; S.O. fabricated the microfluidic devices; A.S., H.K., N.A., M.R., and A.K. wrote the paper.

- <sup>1</sup>J. M. Shulman and P. L. De Jager, *Nat. Genet.* **41**, 1261 (2009).
- <sup>2</sup>P. S. D. Foundation, [http://www.pdf.org/en/parkinson\\_statistics](http://www.pdf.org/en/parkinson_statistics).
- <sup>3</sup>L. S. Forno, *J. Neuropathol. Exp. Neurol.* **55**, 259 (1996).
- <sup>4</sup>M. G. Spillantini, M. L. Schmidt, V. M. Lee, J. Q. Trojanowski, R. Jakes, and M. Goedert, *Nature (London)* **388**, 839 (1997).
- <sup>5</sup>E. Sofic, P. Riederer, H. Heinsen, H. Beckmann, G. P. Reynolds, G. Hebenstreit, and M. B. Youdim, *J. Neural Transm.* **74**, 199 (1988).
- <sup>6</sup>A. M. Gorman, E. Szegezdi, D. J. Quigney, and A. Samali, *Biochem. Biophys. Res. Commun.* **327**, 801 (2005).
- <sup>7</sup>S. B. Berman and T. G. Hastings, *J. Neurochem.* **73**, 1127 (1999).
- <sup>8</sup>S. Fahn, *Ann. Neurol.* **47**, 2 (2000).
- <sup>9</sup>N. J. Hewitt, M. J. Lechon, J. B. Houston, D. Hallifax, H. S. Brown, P. Maurel, J. G. Kenna, L. Gustavsson, C. Lohmann, C. Skonberg, A. Guillouzo, G. Tuschl, A. P. Li, E. LeCluyse, G. M. Groothuis, and J. G. Hengstler, *Drug Metab. Rev.* **39**, 159 (2007).
- <sup>10</sup>A. Manz, N. Graber, and H. M. Widmer, *Sens. Actuators B* **1**, 244 (1990).
- <sup>11</sup>P. Sethu, L. L. Moldawer, M. N. Mindrinos, P. O. Scumpia, C. L. Tannahill, J. Wilhelm, P. A. Efron, B. H. Brownstein, R. G. Tompkins, and M. Toner, *Anal. Chem.* **78**, 5453 (2006).
- <sup>12</sup>S. Moon, H. O. Keles, A. Ozcan, A. Khademhosseini, E. Haeggstrom, D. Kuritzkes, and U. Demirci, *Biosens. Bioelectron.* **24**, 3208 (2009).
- <sup>13</sup>A. Tirella, M. Marano, F. Vozzi, and A. Ahluwalia, *Toxicol. In Vitro* **22**, 1957 (2008).
- <sup>14</sup>Y. Du, J. Shim, M. Vidula, M. J. Hancock, E. Lo, B. G. Chung, J. T. Borenstein, M. Khabiry, D. M. Crokek, and A. Khademhosseini, *Lab Chip* **9**, 761 (2009).
- <sup>15</sup>S. K. Mahto, T. H. Yoon, H. Shin, and S. W. Rhee, *Biomed. Microdevices* **11**, 401 (2009).
- <sup>16</sup>A. Khademhosseini, R. Langer, J. Borenstein, and J. P. Vacanti, *Proc. Natl. Acad. Sci. U.S.A.* **103**, 2480 (2006).
- <sup>17</sup>B. G. Chung and J. Choo, *Electrophoresis* **31**, 3014 (2010).

- <sup>18</sup>L. Kang, B. G. Chung, R. Langer, and A. Khademhosseini, *Drug Discovery Today* **13**, 1 (2008).
- <sup>19</sup>Y. Izumi, H. Sawada, N. Sakka, N. Yamamoto, T. Kume, H. Katsuki, S. Shimohama, and A. Akaike, *J. Neurosci. Res.* **79**, 849 (2005).
- <sup>20</sup>J. He, Y. Du, J. L. Villa-Urbe, C. Hwang, D. Li, and A. Khademhosseini, *Adv. Funct. Mater.* **20**, 131 (2010).
- <sup>21</sup>S. J. Martin, C. P. Reutelingsperger, A. J. McGahon, J. A. Rader, R. C. van Schie, D. M. LaFace, and D. R. Green, *J. Exp. Med.* **182**, 1545 (1995).
- <sup>22</sup>P. Gee and A. J. Davison, *Free Radic. Biol. Med.* **6**, 271 (1989).
- <sup>23</sup>B. Halliwell, *J. Neurochem.* **59**, 1609 (1992).
- <sup>24</sup>Y. Saito, K. Nishio, Y. Ogawa, T. Kinumi, Y. Yoshida, Y. Masuo, and E. Niki, *Free Radic. Biol. Med.* **42**, 675 (2007).
- <sup>25</sup>C. F. Jin, S. R. Shen, Sr., and B. L. Zhao, *J. Agric. Food Chem.* **49**, 6033 (2001).
- <sup>26</sup>G. Walker and D. Beebe, *Lab Chip* **2**, 131 (2002).
- <sup>27</sup>T. Nakazato and A. Akiyama, *Neurochem. Res.* **23**, 1 (1998).
- <sup>28</sup>S. K. W. Dertinger, D. T. Chiu, N. L. Jeon, and G. M. Whitesides, *Anal. Chem.* **73**, 1240 (2001).
- <sup>29</sup>H. Mochizuki, K. Goto, H. Mori, and Y. Mizuno, *J. Neurol. Sci.* **137**, 120 (1996).
- <sup>30</sup>E. E. Ochu, N. J. Rothwell, and C. M. Waters, *J. Neurochem.* **70**, 2637 (1998).
- <sup>31</sup>R. C. Armstrong, T. J. Aja, K. D. Hoang, S. Gaur, X. Bai, E. S. Alnemri, G. Litwack, D. S. Karanewsky, L. C. Fritz, and K. J. Tomaselli, *J. Neurosci.* **17**, 553 (1997).
- <sup>32</sup>Y. Du, R. C. Dodel, K. R. Bales, R. Jemmerson, E. Hamilton-Byrd, and S. M. Paul, *J. Neurochem.* **69**, 1382 (1997).
- <sup>33</sup>Y. Du, K. R. Bales, R. C. Dodel, E. Hamilton-Byrd, J. W. Horn, D. L. Czilli, L. K. Simmons, B. Ni, and S. M. Paul, *Proc. Natl. Acad. Sci. U.S.A.* **94**, 11657 (1997).
- <sup>34</sup>J. Qin, N. Ye, X. Liu, and B. Lin, *Electrophoresis* **26**, 3780 (2005).
- <sup>35</sup>N. Ye, J. Qin, X. Liu, W. Shi, and B. Lin, *Electrophoresis* **28**, 1146 (2007).
- <sup>36</sup>W. Dai, Y. Zheng, K. Luo, and H. Wu, *Biomicrofluidics* **4**, 024101 (2010).